ISSN 1070-3284, Russian Journal of Coordination Chemistry, 2016, Vol. 42, No. 11, pp. 742–748. © Pleiades Publishing, Ltd., 2016.

Synthesis, Structures, and Magnetic Properties of Two Closely-Related Manganese(II) Coordination Polymers[1]

X. L. Li, W. D. Yin, G. Z. Liu*, L. Y. Xin, and G. L. Li

College of Chemistry and Chemical Engineering, Luoyang Normal University, Henan, Luoyang 471022 P.R. China

**e-mail: gzliuly@126.com*

Received November 2, 2015

Abstract—The reactions of Mn^{2+} ion with 4-nitrobenzene-1,2-bicarboxylic acid in the presence of bipyridyl-type coligands gave two new manganese(II) coordination polymers, $[Mn_2(Nbdc)_2(Bipyp)(H_2O)_4]_n$ (**I**) and $[Mn_2(Nbdc)_2(Bipye)(H_2O)_4]_n$ (**II**) (H_2Nbdc = 4-nitrobenzene-1,2-bicarboxylic acid, Bipyp = 1,3-bi(4-pyridyl)propane, and Bipye = 1,2-bi(4-pyridyl)ethane). Both two complexes contain uniform carboxyl-bridged manganese chains with the composition of $[Mn_2(Nbdc)_2(H_2O)_4]_n$, which are interlinked by inter-chain Bipyp/Bipye spacers to afford two closely-related layers (CIF files CCDC nos. 1008182 (**I**) and 1008183 (**II**)). Magnetic studies for two compounds show the presence of similar antiferromagnetic couplings between the adjacent Mn^{2+} ions through the carboxyl bridges, the best fittings to the experimental magnetic susceptibilities gave $J = -0.20$ cm^{-1} and $g = 1.96$ for **I**, and $J = -0.24$ cm^{-1} and $g = 1.98$ for **II**. Similar magnetic parameters and thermal behaviors further verify that two compounds possess closely-related structures.

Keywords: 4-nitrobenzene-1,2-bicarboxylic acid, manganese coordination polymers, magnetic properties

DOI: 10.1134/S1070328416110051

INTRODUCTION

The rapid expanding field of desirable coordination polymers based upon assembly of metal ions and multifunctional organic ligands is of significant interest for their fascinating structural diversities and specific applications in the areas of electrochemistry, photophysics, catalysis, adsorption and separation [1–5]. It is well-known that the basic strategy to design magnetic coordination polymers is to employ appropriate bridging ligands to bind paramagnetic metal centers of specific coordination geometry, which can efficiently propagate magnetic interactions [6–10]. Although phenyldicarboxylates are less efficient superexchange mediator, its diverse binding modes lead to variations in the magnetic properties owing to its orientation with respect to the magnetic centers [11–13]. Moreover, the high-spin Mn(II), which contains five unpaired electrons, is often used to build novel coordination architectures because some of carboxylato-bridged Mn(II) compounds exhibit interesting magnetic properties [14, 15]. Considering that the carboxylate group can also efficiently transmit superexchange, increasing attention has been devoted to the construction of manganese carboxylate frameworks [16, 17]. For example, some workers have adopted 1,2-benzenedicarboxylic acid (1,2-H_2Bdc) to create a series of metal-organic frameworks, where 1,2-H_2Bdc acid can function as a mediator for magnetic exchange between the paramagnetic metal centers [18–21]. On the other hand, the dipyridyl-type ligands, such as 4,4'-bipyridine (Bipy), 1,3bi(4-pyridyl)propane (Bipyp) and 1,2-bi(4-pyridyl)ethane (Bipye), can satisfy and even mediate the overall molecular architectures and consequently generate more meaningful properties, which are dependent on the nature of bipyridyl-type ligands with different carbon backbones between two 4-pyridyl rings. Related results are quite useful for understanding the coordination-driven assembly and recognition process [22–25].

Very recently, our laboratory has adopted a flexible linker 4-nitrobenzene-1,2-bicarboxylic acid (H_2Nbdc), a derivative of 1,2-H_2Bdc, to assemble a series of metal–organic frameworks [26–29]. In comparison with 1,2-H_2Bdc, H_2Nbdc not only contains two carboxylate moieties but also possesses the electron-withdrawing substituent ($-NO_2$) on the benzene backbone, which can further provide the potential to regulate the structures and properties of coordination polymers. We report herein the binding of H_2Nbdc and bpp/bpa ligands to Mn(II) centers forming two layered coordination polymers with closely-related related structures, $[Mn_2(Nbdc)_2(Bipyp)(H_2O)_4]_n$ (**I**) and $[Mn_2(Nbdc)_2(Bipye)(H_2O)_4]_n$ (**II**). Their physical properties, such as IR, PXRD, thermal stabilities, and magnetic properties have also been inves-

[1] The article is published in the original.

tigated. Owing to closely-related layer structures, compounds **I** and **II** have owned similar thermal events and magnetic parameters.

EXPERIMENTAL

Materials and physical measurements. All chemicals for synthesis were of reagent grade and obtained from commercial sources without further purification. Elemental analysis (C, H and N) were performed on a Flash 2000 organic elemental analyzer. Infrared spectra (IR) were recorded on powdered samples using a NICOLET 6700 FT–IR spectrometer over a range 4000–400 cm^{-1}. Thermogravimetric analyses (TGA) were investigated on a SII EXStar6000 TG/DTA6300 analyzer in flowing N_2 with a heating rate of 10 K/min up to 900°C. The powder X-ray diffraction (PXRD) patterns were obtained on a Bruker D8-ADVANCEX ray diffractometer (CuK_α radiation, λ = 1.5418 Å) at room temperature. Variable temperature magnetic susceptibility data were collected on a Quantum Design SQUID MPMS XL-7 instrument in a magnetic field of 2000 Oe. Diamagnetic corrections were made with Pascal's constants for all constituent atoms.

Synthesis of complex I. A mixture of H_2Nbdc (0.1 mmol, 21.2 mg), Bipyp (0.2 mmol, 19.6 mg), $Mn(Ac)_2 \cdot 4H_2O$ (0.1 mmol, 24.9 mg), and H_2O (6.0 mL) was sealed in a 23 mL Teflon-lined autoclave, heated to 120°C for 4 days, then cooled at 5 K/h to room temperature. Colourless block crystals were obtained.

For $C_{29}H_{28}N_4O_{16}Mn_2$

anal. calcd, %:	C, 43.63;	H, 3.53;	N, 7.02.
Found, %:	C, 43.42;	H, 3.68;	N, 7.19.

Synthesis of complex II. A mixture of H_2Nbdc (0.1 mmol, 21.1 mg), Bipye (0.2 mmol, 18.5 mg), $Mn(Ac)_2 \cdot 4H_2O$ (0.1 mmol, 24.5 mg), H_2O (6.0 mL), and KOH (0.1 mmol) were sealed in a 23 mL Teflon-lined autoclave, heated to 120°C for 4 days, then cooled at 5 K/h to room temperature.

For $C_{28}H_{26}N_4O_{16}Mn_2$

anal. calcd, %:	C, 42.87;	H, 3.34;	N, 7.14.
Found, %:	C, 42.70;	H, 3.42;	N, 7.29.

X-ray structure determination. Single-crystal X-ray diffraction data for **I** and **II** were collected on a Bruker SMART APEX CCD diffractometer equipped with graphite-monochromated MoK_α radiation at 296 K. Absorption corrections were based on symmetry equivalent reflections using the multi-scan program SADABS. The structures were solved using direct methods of SHELXS-97 and refined by full-matrix least-squares methods using the SHELXL-97 program. All non-hydrogen atoms of compounds **I** and **II** were refined on F^2 by a full matrix least-squares procedure using anisotropic thermal parameters. The hydrogen atoms were generated geometrically except for those bound to water molecules, which were initially located from difference Fourier maps and refined by use of geometrical restraints. The nitro group (O(5), O(6)) of Nbdc dianion in **I** are highly disordered and some soft constraints were also applied. The crystal data as well as details of data collection and refinements for **I** and **II** are summarized in Table 1. Selected bond lengths and bond angles are listed in Table 2, while hydrogen bond distances and bond angles are listed in Table 3.

Supplementary materials for two compounds have been deposited with Cambridge Crystallographic Data Centre (nos. 1008182 (**I**) and 1008183 (**II**); deposit@ccdc.cam.ac.uk or http://www.ccdc.cam.ac.uk).

RESULTS AND DISCUSSION

Compound **I** exhibits a 2D layer architecture in which 1D Mn(II) chains with carboxylate bridges are linked by Bipyp spacers, further forming the 3D supermolecule structure by the H-bonded interactions. The asymmetric unit of **I** contains one Mn^{2+} ion, one Nbdc anion, half Bipyp molecule and two coordination water molecules, as shown in Fig. 1a. The Mn(II) atom is six-coordinate by three oxygen atoms from two Nbdc dianions, by two coordinated water molecule and one nitrogen atoms from bridging bpp showing a slightly distorted octahedral coordination geometry. All the Mn–O bond lengths are in the range of 2.1403(18)–2.2284(17) Å, and the Mn–N bond distance is 2.258(2) Å, which are comparable to the previously reported values. The nitro group (O(5), O(6)) of Nbdc dianion is disordered over two crystallographic positions.

Coordination mode of H_2Nbdc ligand observed in **I** and **II** can be reprezented as follows:

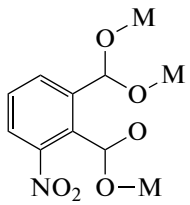

The 1-carboxylate group of Nbdc dianion adopts a $\eta^1{:}\eta^0$ coordination mode to link one Mn(II) atom, while the 2-carboxylate group exhibits a $\eta^1{:}\eta^1$ bridging coordination mode to connect two Mn(II) atoms. Along the *y* direction, the neighboring manganese atoms are bridged by the Nbdc dianions to generate an infinite carboxylate chain, which are interconnected to each other through the Bipyp molecules to result in a 2D layer (Fig. 1b). Multiple hydrogen bonds are known to cooperatively exert influence on the control of molecular self assembly in chemical and biological

Table 1. Crystallographic data and structure refinement parameters for **I** and **II**

Parameter	Value	
	I	**II**
Formula weight	798.43	784.40
Crystal system	Orthorhombic	Monoclinic
Space group	*Aba*2	$P2_1/n$
a, Å	30.125(3)	7.3604(14)
b, Å	9.9186(10)	28.572(6)
c, Å	11.4495(11)	7.5860(15)
β, deg	90	96.882(2)
Volume, Å^3	3421.0(6)	1583.8(5)
Crystal size, mm	0.33 × 0.25 × 0.21	0.35 × 0.28 × 0.27
Z	4	2
ρ_{calcd}, g cm^{-3}	1.550	1.645
μ, mm^{-1}	0.817	0.881
F(000)	1632	800
θ Range, deg	2.70 to 25.50	2.80 to 25.50
Number of reflections measured	10183	11690
unique (*N*) (R_{int})	3134 (0.0240)	2938 (0.0330)
Restraints/parameters	37/241	0/226
GOOF on F^2	1.040	1.063
Final *R* indices ($I > 2\sigma(I)$)	$R_1 = 0.0255$, $wR_2 = 0.0568$	$R_1 = 0.0312$, $wR_2 = 0.0791$
R indices (for *N*)	$R_1 = 0.0285$, $wR_2 = 0.0583$	$R_1 = 0.0393$, $wR_2 = 0.0833$
$\Delta\rho_{max}/\Delta\rho_{min}$, e Å^{-3}	0.207/–0.220	0.392/–0.375

systems. Due to the presences of two coordinated water molecule, there are four kinds of H-bonding interactions in I. There exist intramolecular hydrogen bonds O(7)–H(1*w*)···O(2)$^{\#1}$ (O···O 2.791(2) Å, ∠OHO 150°) in the 2D layers, stabilizing the resulting structure (Fig. 1b). Two adjacent sheets are further connected by the intermolecular hydrogen bonding interactions O(8)–H(4*w*)···O(1)$^{\#4}$ (O···O 2.958(3) Å, ∠OHO 167); O(8)–H(3*w*)···O(4)$^{\#5}$ (O···O 2.708(3) Å, ∠OHO 154°) and O(7)–H(2*w*)···O(4)$^{\#4}$ (O···O 2.627(3) Å, ∠OHO 162°) to produce a entire 3D supramolecular architecture. The intermolecular hydrogen bonds play an important role in creating such a high-dimensional structure.

Compound **II** exhibits similar molecule unit, ligand-metal coordination mode, and layer architecture to that of **I** (Fig. 1c). Concretely, both compounds possess uniform carboxylate chain unit $[Mn_2(Nbdc)_2(H_2O)_4]_n$, nevertheless, the orientation of the chains within the layer has a little distinction because they crystallize in different space groups. In addition, the spacer between the chain motifs is less flexible Bipye molecule for **II** instead of Bipyp molecule for **I**. All these parameters provoke some structure differences between two compounds as described below: (1) The distance between adjacent chain motifs shortens slightly for **II** due to small molecule size for Bipye spacer: molecule length of 9.3284(30) Å for Bipye ligand is slightly shorter than that of 9.9651(31) Å for Bipyp ligand. (2) The structure of **II** has a higher degree of condensation than that of **I** ($d_1 = 1.550$ for **I** < $d_2 = 1.645$ for **II**). (3) Two compounds exhibit very similar hydrogen-bonding interactions with completely identical intralayer hydrogen bonds and slightly different interlayer hydrogen bonds. The intralayer hydrogen bonds are formed by coordination water H atom and carboxylate O atom within the chain motifs for two compounds. The interlayer hydrogen bonds are formed by coordination water H atoms of one layer with carboxlyate O atoms of the adjacent layer for **I**, whereas water H atoms and carboxylate O atoms concerning the interlayer hydrogen

Table 2. Selected bond lengths (Å) and angles (deg) for **I** and **II***

Bond	*d,* Å	Bond	*d*, Å
	I		
Mn(1)–O(3)	2.1403(18)	Mn(1)–O(7)	2.1729(16)
Mn(1)–O(8)	2.1844(19)	Mn(1)–O(1)$^{\#1}$	2.2026(16)
Mn(1)–O(2)	2.2284(17)	Mn(1)–N(2)	2.258(2)
	II		
Mn(1)–O(4)	2.1420(15)	Mn(1)–O(7)	2.1692(17)
Mn(1)–O(8)	2.1746(16)	Mn(1)–O(1)$^{\#1}$	2.2057(15)
Mn(1)–O(2)	2.2363(15)	Mn(1)–N(2)	2.2435(18)
Angle	ω, deg	Angle	ω, deg
	I		
O(3)Mn(1)O(7)	83.97(7)	O(3)Mn(1)O(8)	179.01(8)
O(7)Mn(1)O(8)	96.20(8)	O(3)Mn(1)O(1)$^{\#1}$	94.26(7)
O(7)Mn(1)O(1)$^{\#1}$	86.34(6)	O(8)Mn(1)O(1)$^{\#1}$	86.72(8)
O(3)Mn(1)O(2)	85.19(6)	O(7)Mn(1)O(2)	166.61(8)
O(8)Mn(1)O(2)	94.77(7)	O(1)$^{\#1}$Mn(1)O(2)	86.66(6)
O(3)Mn(1)N(2)	91.65(8)	O(7)Mn(1)N(2)	92.32(7)
O(8)Mn(1)N(2)	87.37(8)	O(1)$^{\#1}$Mn(1)N(2)	173.77(8)
O(2)Mn(1)N(2)	95.82(7)		
	II		
O(4)Mn(1)O(7)	176.03(7)	O(4)Mn(1)O(8)	85.36(6)
O(7)Mn(1)O(8)	95.97(7)	O(4)Mn(1)O(1)$^{\#1}$	97.03(6)
O(7)Mn(1)O(1)$^{\#1}$	86.81(7)	O(8)Mn(1)O(1)$^{\#1}$	85.73(6)
O(4)Mn(1)O(2)	84.40(6)	O(7)Mn(1)O(2)	94.81(7)
O(8)Mn(1)O(2)	166.77(6)	O(1)$^{\#1}$Mn(1)O(2)	87.24(6)
O(4)Mn(1)N(2)	89.37(6)	O(7)Mn(1)N(2)	86.88(7)
O(8)Mn(1)N(2)	90.40(7)	O(1)$^{\#1}$Mn(1)N(2)	172.22(6)
O(2)Mn(1)N(2)	97.83(6)		

* Symmetry codes: $^{\#1}$ $-x + 1/2, y - 1/2, z$ (**I**); $^{\#1}$ $x - 1/2, -y + 1/2, z - 1/2$ (**II**).

bonds are mutually provided by two adjacent layers in **II** (Fig. 2).

Thermal degenerations of two complexes have been investigated through TG experiments in order to probe the thermal stabilities of their 3D supramolecular networks. The TGA for **I** and **II** shows that two compound**s** display almost similar thermal behaviors resulting from their intimately-related structures. The mass was unchanged until ~120°C, at which point combustion of the coordination water molecules ensued. The mass loss (8.81% for **I**, 8.89% for **II**) between 120 and 180°C corresponds reasonably well to escape of the coordination water molecules (calcd. 9.03% for **I**, 9.19% for **II**). And then weight loss of the organic ligands for two compounds proceeded until 900°C.

The purity of complexes **I** and **II** was confirmed by PXRD analysis. The experimental PXRD patterns of two compounds are consistent well with the patterns simulated from the respective single-crystal data, confirming the bulk purity of the two samples. Though two compounds possess two closely-related layer structures, the PXRD pattern of **I** is slightly different from that of **II** owing to the nature of the auxiliary Bipyp/Bipye ligands.

The variable-temperature magnetic susceptibilities of **I** and **II** were measured under an applied field of 2000 Oe over the temperature range 2–300 K. The χ_M and $\chi_M T$ vs. T plots are shown in Fig. 3. The $\chi_M T$ values per Mn(II) for **I** and **II** at 300 K are about 4.21 and 4.25 cm^3 K mol^{-1}, respectively, which are close to the spin-only value (4.38 cm^3 K mol^{-1}) expected for a

Table 3. Geometric parmeters of hydrogen bonds for compounds **I** and **II***

D–H···A	Distance, Å			Angle DHA, deg
	D–H	H···A	D···A	
		I		
O(8)–H(4*w*)···O(1)$^{\#2}$	0.85	2.12	2.958(3)	167.1
O(8)–H(3*w*)···O(4)$^{\#3}$	0.85	1.92	2.708(3)	154.0
O(7)–H(2*w*)···O(4)$^{\#2}$	0.85	1.81	2.627(3)	161.5
O(7)–H(1*w*)···O(2)$^{\#1}$	0.85	2.02	2.791(2)	149.6
		II		
O(7)–H(1*w*)···O(1)$^{\#2}$	0.85	2.15	2.914(2)	150.0
O(7)–H(2*w*)···O(3)$^{\#3}$	0.85	1.89	2.726(2)	167.7
O(8)–H(3*w*)···O(2)$^{\#1}$	0.85	1.95	2.742(2)	153.6
O(8)–H(4*w*)···O(3)$^{\#2}$	0.85	1.83	2.657(2)	162.8

* Symmetry codes: $^{\#1}$ $-x + 1/2, y - 1/2, z$; $^{\#2}$ $x, y - 1/2, z + 1/2$; $^{\#3}$ $-x + 1/2, y + 0, z + 1/2$ (**I**); $^{\#1}$ $x - 1/2, -y + 1/2, z - 1/2$; $^{\#2}$ $x, y, z - 1$; $^{\#3}$ $x + 1/2, -y + 1/2, z - 1/2$.

magnetically isolated high-spin Mn(II) center (S_{Mn} = 5/2, g = 2). When the system is cooled down, the $\chi_M T$ value undergoes a gradual decrease down to 1.73 cm^3 K mol^{-1} at 2 K for **I** and 1.65 cm^3 K mol^{-1} at 2 K for **II**. It was found that the magnetic susceptibility of two compounds obeys the Curie–Weiss law perfectly: C = 4.24 cm^3 K mol^{-1}, θ = –2.15 K for **I** and C = 4.31 cm^3 K mol^{-1}, θ = –2.39 K for **II**, respectively. The negative θ values in two compounds suggest the antiferromagnetic interactions within the neighbour-

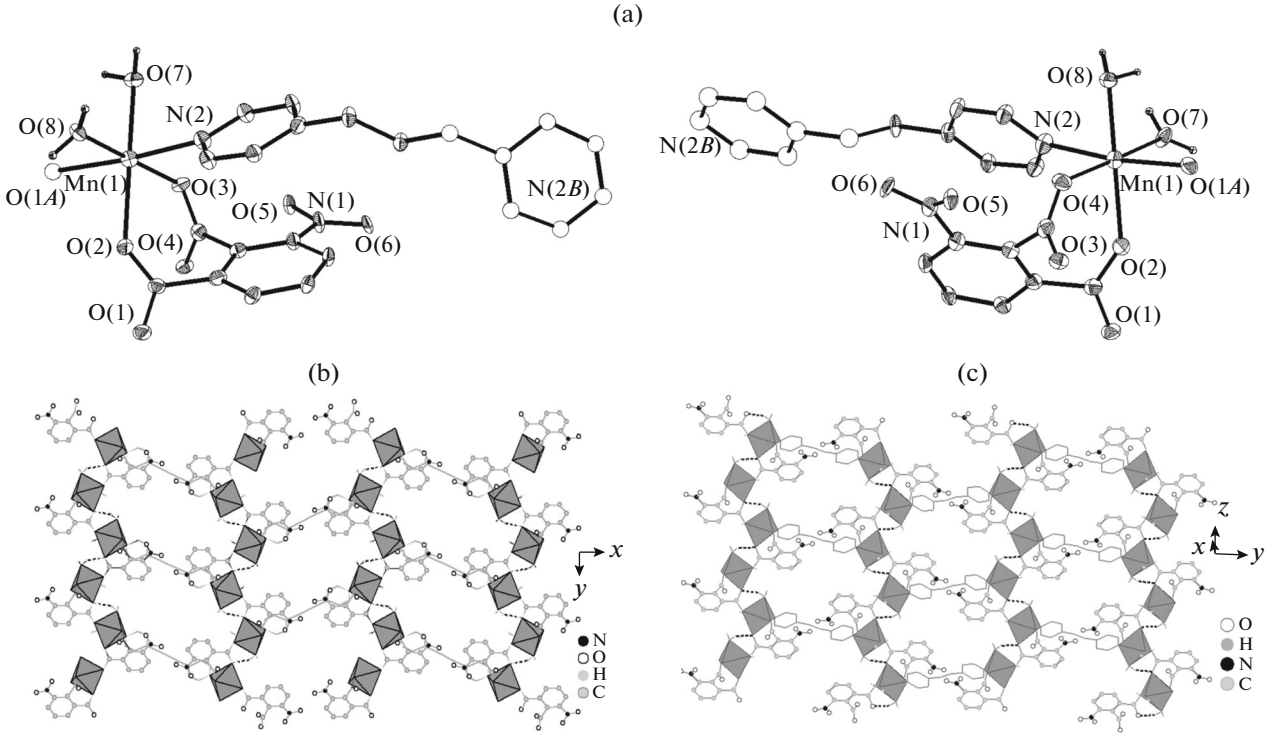

Fig. 1. ORTEP plot of the asymmetric unit showing the coordination environment of Mn(II) center for **I** (left) and **II** (right). Symmetry codes: (*A*) 0.5 – *x*, –0.5 + *y*, *z*; (*B*) –*x*, 1 – *y*, *z* for **I** and (*A*) *x* – 0.5, –*y* + 0.5, *z* – 0.5; (*B*) –*x* + 2, –*y*, –*z* for **II** (a). Schematic representation of a 2D layer along the *xy* plane for **I** (b). View of the 2D layer parallel to *yz* plane for **II** (c). Dotted line represents the interlayer hydrogen bonds within the layer.

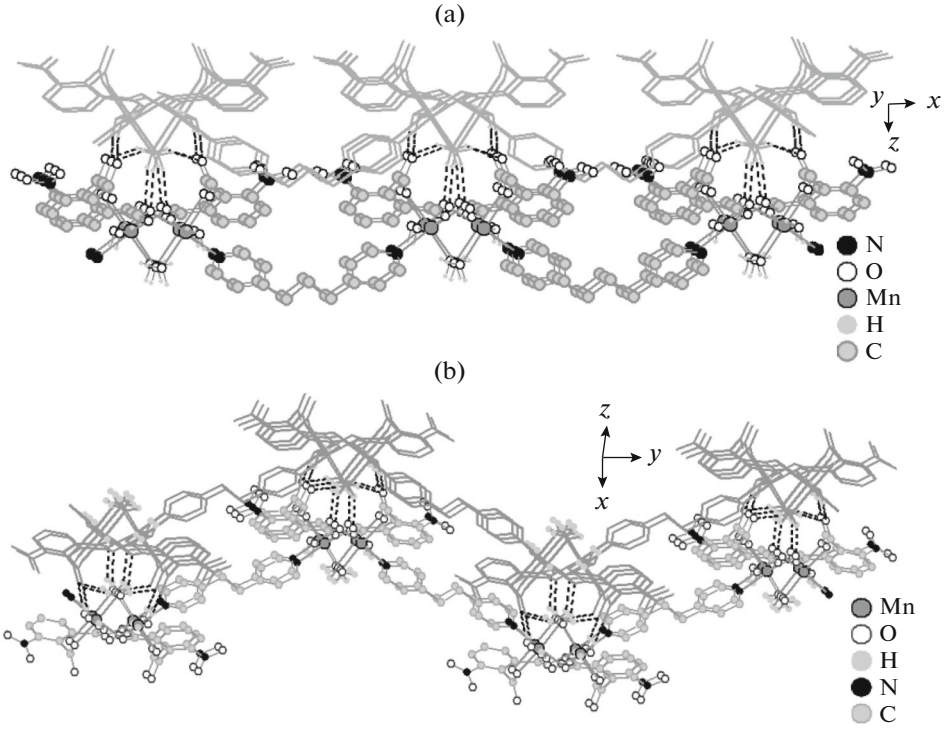

Fig. 2. Interactions of H-bonds exist in-between two neighboring layers for **I** (a) and **II** (b).

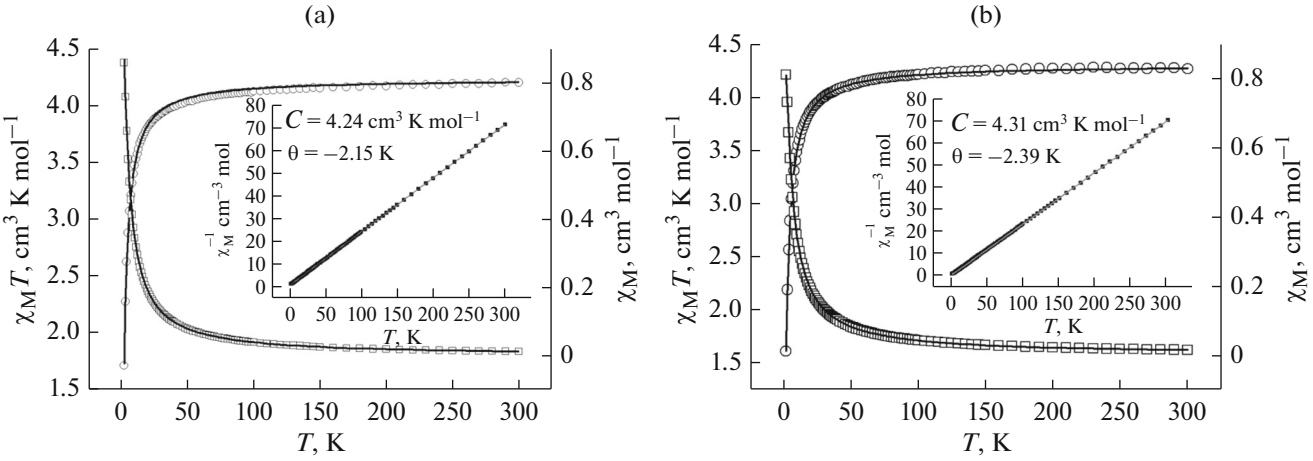

Fig. 3. Temperature dependence of χ_M and $\chi_M T$ for **I** (a) and **II** (b) and their corresponding theoretical curves (solid lines).

ing Mn^{2+} metal ions. Obviously, the magnetic interactions between Mn^{2+} ions in two compounds primarily have been transmitted by the Nbdc-bridge, whereas the coupling between Mn^{2+} ions through Bipyp/Bipye-bridge can be ignored due to the long distance. Compound **II** has similar magnetic curve as that of **I**, suggesting that two compounds afford two closely-related layers.

From a magnetic point of view, the magnetic susceptibilities of two compounds can be considered as pseudo-1D chain model, derived from the exchange spin Hamiltonian 1D chain:

$$\chi_{chain} = [Ng^2\beta^2S(S+1)/3kT][(1+u)/(1-u)],$$

where u is the Langevin function $u = \coth[JS(S+1)/kT] - [kT/JS(S+1)]$, and N, β, K, g, and T bear their usual meanings.

The least-squares analysis of the magnetic susceptibility data lead to $J = -0.20$ cm^{-1}, $g = 1.96$ and $R = 2.8 \times 10^{-5}$ for **I** and $J = -0.24$ cm^{-1}, $g = 1.98$ and $R =$

2.5×10^{-6} for **II**. The negative coupling constant J in **I** and **II** also indicate that there exist weak antiferromagentic exchange coupling between the two Mn^{2+} ions bridged by carboxylate groups.

In this contribution, in order to understand the influence of H_2Nbdc with different dipyridyl-type ligands on the assembly of MOFs, we successfully have obtained two closely-related Mn(II) coordination polymers with uniform carboxyl-bridged manganese chains bearing different dipyridyl-type ligands. The structural disparity for two compounds is mainly attributed to the nature of the spacers ($-CH_2CH_2CH_2-$ and $-CH_2CH_2-$) between two 4-pyridyl rings in Bipye/Bipyp. The different orientation of intermolecular hydrogen bonds in **I** and **II**, which linked the adjacent layers, probably has been spurred by different space group. The magnetic curve profiles for two compounds have revealed that the H_2Nbdc bridges in two compounds induce antiferromagnetic couplings between the neighboring Mn(II) centers, whereas the couplings through the Bipyp/Bipye bridges can be ignored due to the long distance. Obviously owing to their intimately-related structures, both compounds have similar thermal events and magnetic properties, which are independent of the dipyridyl-type ligands (Bipyp/Bipye).

ACKNOWLEDGMENTS

This work was supported by the National Natural Science Foundation of China (no. 21571093), the Program for Science and Technology Innovation Talents in Universities of Henan Province (no. 14HASTIT017), the Program for Innovative Research Team (in Science and Technology) in University of Henan Province (no. 14IRTSTHN008) and the Foundation of Education Committee of Henan Province (nos. 142300410301 and 15A150063).

REFERENCES

1. Sumida, K., Brown, C.M., Herm, Z.R., et al., *Chem. Commun.*, 2011, vol. 47, no. 4, p. 1157.
2. Du, L., Lu, Z., Zheng, K., et al., *J. Am. Chem. Soc.*, 2013, vol. 135, no. 2, p. 562.
3. Avendano, C., Zhang, Z.Y., Ota, A., et al., *Angew. Chem. Int. Ed.*, 2011, vol. 50, no. 29, p. 6543.
4. Song, Y.M., Luo, F., and Luo, M.B., et al., *Chem. Commun.*, 2012, vol. 48, no. 7, p. 1006.
5. Pérez-Yañez, S., Beobide, G., Castillo, O., et al., *Cryst. Growth Des.*, 2013, vol. 13, no. 7, p. 3057.
6. Escuer, A. and Aromí, G., *Eur. J. Inorg. Chem.*, 2006, no. 23, p. 4721.
7. Zeng, Y.F., Hu, X., Liu, F.C., et al., *Chem. Soc. Rev.*, 2009, vol. 38, no. 2, p. 469.
8. Wang, Y.Q., Jia, Q.X., Wang, K., et al., *Inorg. Chem.*, 2010, vol. 49, no. 4, p. 1551.
9. Zhang, F.W., Li, Z.F., Ge, T.Z., et al., *Inorg. Chem.*, 2010, vol. 49, no. 8, p. 3776.
10. Zhang, Y., Wang, X.T., Zhang, X.M., et al., *Inorg. Chem.*, 2010, vol. 49, no. 13, p. 5868.
11. Xanthopulos, C.E., Sigalas, M.P., Katsoulos, G.A., et al., *Inorg. Chem.*, 1993, vol. 32, no. 24, p. 5433.
12. Hong, C.S., Son, S.K., Lee, Y.S., et al., *Inorg. Chem.*, 1999, vol. 38, no. 24, p. 5602.
13. Wang, R.H., Yuan, D.Q., Jiang, F.L., et al., *Eur. J. Inorg. Chem.*, 2006, no. 8, p. 1649.
14. Wang, L., Zhao, R., Xu, L.Y., et al., *CrystEngComm*, 2014, vol. 16, no. 7, p. 2070.
15. Ma, L.F., Wang, L.Y., Wang, Y.Y., et al., *CrystEngComm*, 2009, vol. 11, no. 1, p. 109.
16. Delgado, F.S., Kerbellec, N., Ruiz-Peréz, C., et al., *Inorg. Chem.*, 2006, vol. 45, no. 3, p. 1012.
17. Gómez, V., Corbella, M., Font-Bardia, M., et al., *Dalton Trans.*, 2010, vol. 39, no. 48, p. 11664.
18. Köferstein, R. and Robl, C., *Z. Anorg. Allg. Chem.*, 2007, vol. 633, no. 8, p. 1127.
19. Ma, C.B., Wang, W.G., Zhang, X.F., et al., *Eur. J. Inorg. Chem.*, 2004, no. 17, p. 3522.
20. Ma, C.B., Chen, C.N., Liu, Q.T., et al., *New J. Chem.*, 2003, vol. 27, no. 5, p. 890.
21. Li, Y.M., Xiao, C.Y., Zhang, X.D., et al., *CrystEngComm*, 2013, vol. 15, no. 38, p. 7756.
22. Cheetham, A.K., Rao, C.N.R., and Feller, R.K., *Chem. Commun.*, 2006, no. 46, p. 4780.
23. Bradshaw, D., Prior, T.J., Cussen, E.J., et al., *J. Am. Chem. Soc.*, 2004, vol. 126, no. 19, p. 6106.
24. Lu, W.G., Jiang, L., and Lu, T.B., *Cryst. Growth Des.*, 2008, vol. 8, no. 1, p. 986.
25. Wang, H.Y., Gao, S., Huo, L.H., et al., *Cryst. Growth Des.*, 2008, vol. 8, no. 2, p. 665.
26. Li, G.L., Liu, G.Z., Ma, L.F., et al., *Chem. Commun.*, 2014, vol. 50, no. 20, p. 2615.
27. Li, G.L., Yin, W.D., Liu, G.Z., et al., *Inorg. Chem. Commun.*, 2014, vol. 43, p. 165.
28. Li, G.L., Liu, G.Z., Huang, L.L., et al., *J. Inorg. Organomet. Polym.*, 2014, vol. 24, no. 3, p. 617.
29. Li, G.L., Liu, G.Z., Xin, L.Y., et al., *Chin. J. Struct. Chem.*, 2014, vol. 33, no. 5, p. 764.